Jurnal Kejuruteraan 12 (1998) 81-98

IGBT Modelling Using Hspice Curve-Fitting Optimisation Method

Norman bin Mariun, Ishak bin Aris,
D. Liang & W. Shepherd

ABSTRACT

This paper presents the development of the IGBT model using the HSPICE package running on a Sun Workstation. The two important characteristics of an IGBT, which were considered in modelling the device, are the conduction (static) and the switching (dynamic) characteristics. The IGBT model proposed is discussed briefly to give background before a detailed development of the model is presented. The steps in modelling the IGBT using the curve-fitting optimisation method available within HSPICE are explained. The simulation results of varying the model parameters are discussed. On the basis of these results appropriate parameters for the IGBT model are determined for use in the curve-fitting optimisation method. Further, the test circuit simulation is presented to validate the static and dynamic parameters of the model chosen. The results are compared with manufacturer's data sheet for the static parameter and laboratory test results for the dynamic parameters. The results are found to be in good agreement.

ABSTRAK

Kertas kerja ini membentangkan pembangunan model IGBT menggunakan perisian HSPICE pada Sun Workstation. Dua ciri IGBT yang penting yang perlu dipertimbangkan dalam permodelan peranti ini adalah ciri pengaliran (statik) dan pensuisan (dinamik). Model IGBT yang dicadangkan dibincang secara ringkas untuk memberi latar belakang sebelum perincian pembangunan dibentangkan. Langkah-langkah permodelan IGBT menggunakan kaedah pengoptimuman pemadanan lengkung terdapat dalam pekej HSPICE diterangkan. Keputusan penyelakuan dengan mengubah parameter model dibincangkan. Berlandaskan keputusan ini parameter yang bersesuaian bagi model IGBT ditentukan dalam penggunaan kaedah pengoptimuman pemadanan lengkung. Seterusnya, penyelakuan litar ujian dibentangkan untuk mengesahkan parameter statik dan dinamik yang dipilih untuk model. Keputusan dibandingkan dengan data dari pembuat bagi parameter statik dan dengan keputusan makmal bagi parameter dinamik. Keputusan didapati mencapai kesamaan.

INTRODUCTION

The importance of Insulated Gate Bipolar Transistor, IGBT (Kaplan 1998) in the power and industrial electronics industries is generally accepted and becoming widely used. Even though it is a relatively new device, the need to model it in SPICE or one of its family is immensely important. Furthermore, for the development of a knowledge based expert system, PECT II (Mariun, 1997) which is based on PECT (Cumbi et al. 1996) the power semiconductor data base can be expanded and its usage enhanced by the inclusion of this new device model representation.

For medium power applications IGBTs are generally chosen for their low saturation voltage, which reduces the power dissipation, resulting in a smaller heat sink and other cooling requirements. Voltage controlled input using IGBTs reduces drive hardware requirements, simplifying circuit complexity and potentially reducing costs. Compared with solutions using bipolar transistors, IGBTs offer good thermal stability, not exhibiting the 'runaway' behaviour associated with some transistor types. Like MOSFETs, power ratings can be enhanced by the use of a parallel connection, but IGBTs are regarded as being more rugged than power MOSFETs. The availability of faster switching speeds that are very close to power MOSFETs (Baliga et al. 1984; Clemente et al. 1991) has also broadened the range of applications for this class of device into many systems, including those in low noise environments.

Several analytical models have been proposed to describe the operating characteristics of the IGBT (Yilmaz 1985; Hefner 1990, 1991, 1994). These models have been implemented on specific simulation programs developed from high level programming languages like FORTRAN. Since there is no facility to access and modify the HSPICE program it is not possible to implement these models directly into HSPICE. A review of power semiconductors for SPICE (Lauritzen 1988) also revealed that there are no IGBT generic models in HSPICE and nor in the discrete component library. Thus the development of a simple model based on the two discrete device generic models, the BJT and MOSFET, which are available on HSPICE was undertaken for this investigation.

This paper presents the development of the IGBT model using the HSPICE package running on a Sun Workstation. The IGBT structure and operating principle are discussed briefly to give background before a detailed development of the model is presented. The results of variation of the model parameters are discussed. On the basis of these results appropriate parameters for the IGBT model are determined for use in the curve-fitting optimisation method available in HSPICE. Further, the test circuit simulation is presented to validate the model parameters chosen.

IGBT CHARACTERISTICS

Figure 1 shows a common symbol of the IGBT and its equivalent circuit (Baliga et al. 1984; Yilmaz et al. 1985). The two important characteristics of an IGBT that was considered in modelling the device are the conduction and the switching characteristics. The conduction characteristic determines the

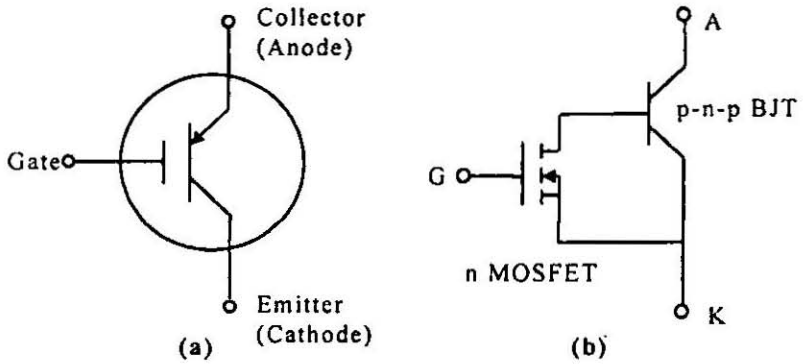

FIGURE 1(a). IGBT Symbol, and (b) IGBT Model

voltage across the collector and the emitter, Vce(on) which is the key rating in calculating the on-state losses. The switching characteristic determines the switching losses which are characterised by the rise time and the fall time.

CONDUCTION CHARACTERISTICS

It is apparent from the equivalent circuit of Figure 1b, that the voltage drop across the IGBT is the sum of two devices. There is a diode across the p-n junction and the voltage drop across an IGBT never goes below a diode threshold. The voltage drop across the driving MOSFET has one characteristic that is typical of all low voltage MOSFETs: it is sensitive to gate drive voltage. This can be observed from Figure 2 where, for currents that are close to their rated value, an increase in gate voltage causes a reduction in the collector-to-emitter voltage. This is due to the fact that, within its operating range, the gain of the p-n-p BJT increases with current and an increase in gate voltage causes an increase in the channel current and hence a reduction in voltage drop across the p-n-p BJT.

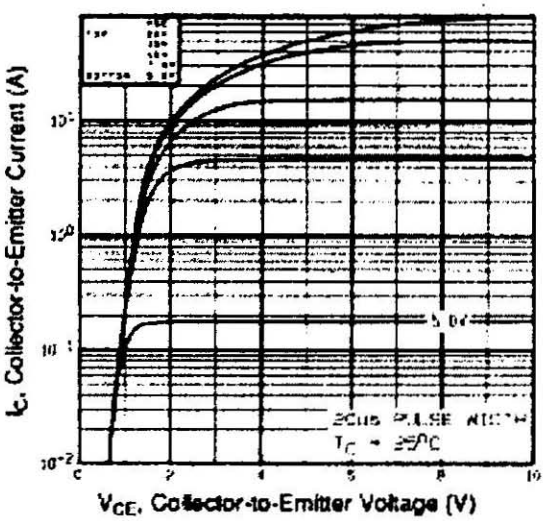

FIGURE 2. Output Characteristics, T_c= 25°C for IGBT IRGBC20F

The p-n-p BJT acts as the final stage of a pseudo-Darlington. It is never in heavy saturation and its voltage drop is higher than what could be obtained from the same p-n-p BJT in heavy saturation. However, the emitter of an IGBT covers the whole area of the die, hence its injection efficiency and conduction drop are much superior to that of a bipolar transistor of the same size.

SWITCHING CHARACTERISTICS

The IGBT is designed such that the turn-on and turn-off times of the device are affected by the gate-to-emitter source impedance. Its equivalent input capacitance is lower than a Power MOSFET with a comparable current and voltage rating. The device is turned on by applying a positive voltage between the gate and the emitter, V_{GE}. In switching applications $V_{GE} >> V_{GE(th)}$, and the device operates in the saturation region.

The device is similar to a Power MOSFET during turn-on and similar to Power Bipolars during turn-off. The biggest limitation to the turn-off speed of an IGBT is the lifetime of the minority carriers in the n- epitaxial layer that is the base of the p-n-p BJT. Since this base is not accessible, external drive circuitry cannot be used to improve the switching time. Since the p-n-p BJT is in pseudo-Darlington connection, it has no storage time and its turn-off time is much better than the same p-n-p BJT in heavy saturation. The charges stored in the base cause the characteristic 'tail' in the current waveform of the IGBT at turn-off. As the MOSFET channel stops conducting, electron current ceases and the IGBT current drops rapidly to the level of the hole recombination current at the inception of the tail. This tail increases turn-off losses and requires an increase in the dead-time between the conduction of two devices in a half bridge which may distort the waveform. For the IGBT IRGBC20F used in this work, the switching times are: t_{don} is 0.025 μs, t_r is 0.018 μs, t_{doff} 0.210 μs, and t_f is 0.600 μs.

THE IGBT MODEL

In developing a model representation of the IGBT, the relevant parameters of the BJT and MOSFET discrete devices and their values have to be determined. The proposed IGBT model, being two discrete devices cascade connected, has more than 100 parameters. Hence, for simplicity, this requires an understanding of the BJT and MOSFET devices model parameters so that some of the parameters can be eliminated where possible in realising a satisfactory model without affecting the characteristics of the device. Further, the relevant parameters that determine the conduction and switching characteristics can be investigated and the values determined to give corresponding characteristics, as specified by the manufacturer's data.

THE HSPICE BJT MODEL

The BJT model in HSPICE is an adaptation of the classic integral charge control model of Gummel and Poon. The HSPICE model extends the original Gummel-Poon model to include several effects at high bias levels. This

model automatically simplifies to the Ebers-Moll model when certain parameters are not specified.

The BJT model used in the IGBT model is a p-n-p BJT due to the IGBT structure. The operation of a p-n-p device is similar in every respect to the n-p-n device if the roles of holes and electrons are interchanged and the polarity of the terminal currents and voltages are reversed.

There are more than 40 parameters for the basic DC model and these can be specified in the model control line for a BJT, as listed in Appendix 1 (Banzhaf 1989; Rashid 1990). In addition there are more than 60 temperature effect parameters that are not considered in this exercise for the sake of simplicity. The basic DC model parameters are divided into several groups, as shown in Table 1.

TABLE 1. BJT model parameters grouping

Group	Parameters
DC	BF BR IBC IBE IS IS NF NR NS VAF VAR
Geometric	SUBS BULK
BETA Degradation	ISC ISE NC NE IKF IKR
Resistance	RB RBM RE RD IRB
Junction Capacitor	CJC CJE CJS FC MJC MJS VJC VJE VJS XCJC
Parasitic Capacitor	CBCP CBEP CCSP
Transit Time	ITF PTF TF VT VTF XTF
Noise	KF AF

The geometric model parameters need not be specified because they will be set appropriately to the default values and, for high current switching applications, the noise parameters can also be ignored. Furthermore, both the Ebers-Moll and Gummel-Poon models are symmetrical, for both forward and reverse operation. Therefore there are forward and reverse parameters that are explicitly labelled as such. However, some of the parameters labelled as being associated with the base-emitter or base-collector junction are also forward or reverse bias parameters. This means that of the forty odd parameters in the bipolar model, most are duplicates, merely specifying reverse operation characteristics which also can be excluded since as a switching device the IGBT operates in the forward region.

From Table 1 the significant static and dynamic parameters of the BJT to be determined for the conduction and switching characteristics are as follows;

static parameters: IS, BF, NF, ISE, NE, IKF, VAF, RB, RE, RC,
dynamic parameters: CJC, CJE, CJS, FC, XCJC, TF, XTF, ITF, VTF, PTF.

THE HSPICE MOSFET MODEL

HSPICE presents an extensive range of models and parameter control techniques for the MOSFET. The models can be specified for either p-channel or n-channel types. For the IGBT model, the n-channel type MOSFET model is used, as defined in the structure of the IGBT, and conduction is maintained

by the electrons in the channel. The carriers are attracted to the surface by the gate voltage and hence the device is called the enhancement MOSFET.

There are 10 levels that can be selected to model the MOSFET. The selection of the MOSFET model type for use in analysis depends on the electrical parameters critical to the application. Two submodels may also be selected. The CAPOP model parameters specify the model for the MOSFET gate capacitances and the ACM parameter selects the type of diode model to be used for MOSFET bulk diodes (Meta-Software 1990).

Level 1 (Schichman-Hodge) models, are often used for simulation where detailed analogue models are not needed (Rashid 1990). They offer low simulation time and a relatively high level of accuracy with regard to timing calculations. They are normally used for large devices (discrete parts, such as signal MOSFETs and power MOSFETs) (Tuinenga 1988). Thus in the following discussion the other levels are not discussed. HSPICE uses three equivalent circuits in the analysis of MOSFETs: DC and transient, AC and noise equivalent circuits. The equivalent circuit for DC sweep is the same as the one used for transient analysis, except that capacitances are not included.

The list of model parameters for the HSPICE MOSFET device is exhaustive. Appendix 2 gives some important parameters for the Level 1 model excluding the temperature effects parameter. These are then grouped as shown in Table 2.

TABLE 2. MOSFET model parameters grouping

Grouping	Parameters
DC	ACM JSW IS N NDS
Capacitance	CBD CBS CJ CJSW FC MJ MJSW NSUB PB PHP TT
Resistance	RD RDC RS RSC RSH
Geometry	LD LMLT WD WMLT XJ XL XW
Threshold Voltage	GAMMA NFS NSUB PHI VTO
Impact Ionisation	ALPHA VCR
Basic	COX LEVEL KP LAMBDA TOX UO
Overlap Capacitance	CGBO CGDO CGSO METO
Noise	AF KF NLEV

Like the BJT model, for simplicity the temperature effects parameters of the MOSFET device are not considered together with the impact ionisation parameters. The noise parameters, for the same reason as the BJT model, are also excluded. Basically the DC and the geometric parameters are used by HSPICE to calculate other parameters.

In this section, it is concluded that the significant static and dynamic parameters to be determined for the MOSFET device model are as listed below;

static parameters: VTO, KP, LAMBDA, PHI, GAMMA, RS, RD,
dynamic parameters: CGDO, CGBO, CGSO, CBD, and CBS.

DETERMINING THE IGBT MODEL PARAMETERS

The model parameters determine the characteristics and performance of the model. Normally for discrete device models of BJT and MOSFET devices, the input model parameters can be evaluated or measured directly from the nodes of the device. There are also techniques to extract the parameters from the manufacturer's data sheet, eliminating the need for actual device measurement (Antognetti 1988; Malik 1990).

In the case of the IGBT model, the techniques mentioned above are impractical, since the device is based on two discrete devices cascade connected. The model parameter evaluation is difficult because of two-dimensional current flow and measurement is impossible because of the inaccessibility of internal nodes. Another alternative to obtain the model parameters for the two discrete devices is by using the curve-fitting optimisation method available with HSPICE. This task can be simplified by optimising only the selected relevant model parameters that determined the conduction and the switching characteristics.

The optimisation method in HSPICE can generate automatically the model parameters and component values from a given set of electrical specifications or measured data. With a user defined optimisation program and a known circuit topology, the design components and model parameters are automatically selected to meet DC, AC, and transient specifications. The optimisation process requires that the user create an input netlist file specifying: the circuit model, circuit parameters which are going to be optimised, minimum and maximum values of the parameters, an initial guess to the selected parameters and components, and the circuit performance goals or model-versus-data error function .

Given the input netlist file, optimisation specifications, parameter limits, and initial estimated values, the optimiser reiterates the circuit simulation until the target electrical specification is met or an optimised solution is found. For improved optimisation and simulation time, and to increase the chance of convergent solution, the initial estimate of the parameter values should produce a circuit with specifications near those of the original target. This reduces the number of times the optimiser reselects parameter values and resimulates the circuit.

Figure 4 and Figure 5 depict the circuits used for simulating the output characteristics and the transient characteristics respectively. These are typical manufacturer's test circuits in obtaining the characteristics from the test bench. The plots are obtained by using the HSPLOT facility available within the HSPICE software.

The static model parameters are determined before the dynamic model parameters to give more meaningful results. The following steps are adopted in determining the model parameters: initial parameters variation tests to determine the typical initial estimate, the lower limit and the upper limit of the parameters for the optimisation method, initial optimisation for obtaining the typical value of the parameters, selected parameter variation tests to determine the effects of the parameters on the characteristics and hence a better initial estimate, lower limit and upper limit can be use, and improved estimate optimisation to determine more accurate model parameters.

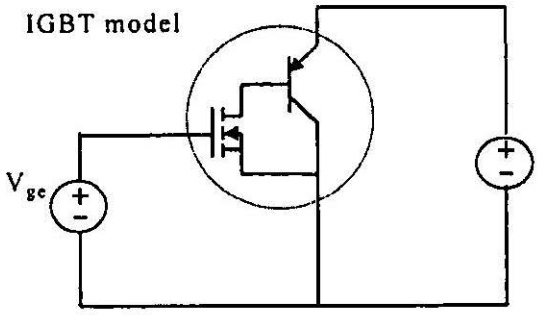

FIGURE 4. Circuit for output characteristics simulation

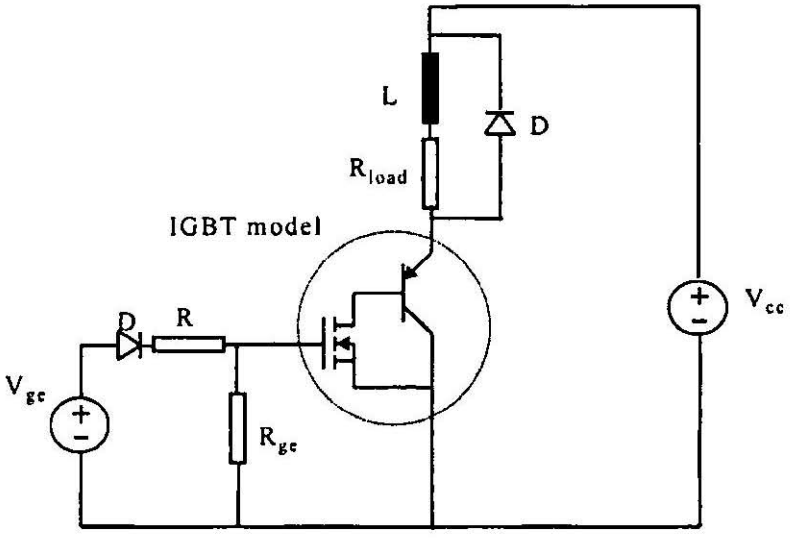

FIGURE 5. Circuit for transient characteristics simulation and test

STATIC PARAMETERS

Table 3 gives the default values and typical values of each of the static parameters considered from the previous section. Using the default and typical parameters gave a low current in general, having maximum value of about 0.1 A for VGE at 15 V. This is expected because the discrete device parameters are for low power devices.

To obtain a good initial estimate for the optimisation method a variation test was carried out. The initial variation for each of the static parameters is carried out by varying separately for a specific range using three different values, as given in Table 3, with the other parameters left at default values. These three values represent typical parameter values with lower and the upper limits which give convergent results. Conduction characteristics curves are plotted for three different values of V_{GE} at 5 V, 10 V and 15 V.

Based on the result of the initial variation tests the initial estimate, the lower limit and the upper limit of each parameter is selected for the initial optimisation. All the static model parameters are optimised. The options of

TABLE 3. Typical values, default values and the values used for variation test

Parameter	Default Values	Typical Value	Variation Values
IS	1e-16	1e-16	1e-16,1e-25, 1e-10
BF	100	10 to 1000	100, 10, 500
NF	1	1	1.0, 0.5, 1.4
ISE	0	100 to 1000	1e-14, 1e-25, 1e-10
NE	1.5	2-4	2, 0.5, 5
IKF	0	0.01 to 0.1	0.01, 0.001, 10
VAF	0	100	100, 10, 500
RB	0	100	100, 1, 500
RE	0	1	10, 0.01, 100
RC	0	10	10, 0.01, 100
VTO	0	1	3, 1, 7
KP	2.0718e-5	2.5e-5	2.5e-6, 1e-6, 1e-4
LAMBDA	0	0.02	0.02, 0.001, 1.0
PHI	0.576	0.625	0.625, 0.1, 1.0
GAMMA	0.5276	0.35	0.35, 0.1, 10
RS	0	1 to 10	0.1, 0.001, 10
RD	0	1 to 10	0.1, 0.001, 10

the model control line should be chosen carefully for a successful convergent simulation.

Based on the result of the initial variation tests the initial estimate, the lower limit and the upper limit of each parameter is selected for the initial optimisation. All the static model parameters are optimised. The options of the model control line should be chosen carefully for a successful convergent simulation.

TABLE 4. Static parameters initial optimisation

Parameter	Initial estimate, lower limit, upper limit	Optimisedvalue
IS	le-15, le-20, le-10	659.0406f
BF	100, 10, 500	500.0
NF	1.0, 0.5, 1.4	938.7808m
ISE	le-14, le-25, le10	1.0693p
NE	2, 1,4	1.2616
IKF	0.1, 0.001, 100	99.9967
VAF	100, 10, 500	126.5610
RB	10, 1, 50	49,9993
RE	0.I, 0.001, 100	1.0m
RC	0.1, 0.001, 100	1.0m
VTO	4, 1, 7	2.6654
KP	2.5e-5, le-6, le-4	88.5975u
LAMBDA	0.01, 0.001, 0.1	80.7726m
PHI	0.5, 0.1, 1.0	607.0191m
GAMMA	0.5, 0.1, 1.0	986.1898m
RS	0.1, 0.001, 100	10.0m
RD	0.1, 0.001, 100	99.9993

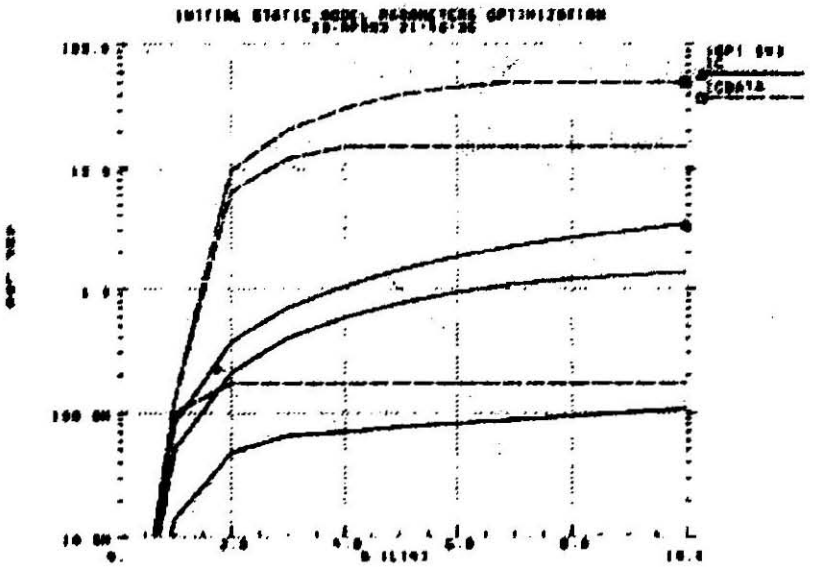

FIGURE 6. Conduction characteristics with static parameter initially optimised

Table 4 lists the values of the static model parameters used for the initial optimisation and the optimised values, while Figure 6 presents the conduction characteristics with the initially optimised model parameters. The results show that the gradient of the saturation region is low compared with the manufacturer's measured data and overall the slope of the active region is steep. Furthermore, the optimised collector current is low against the desired value. Hence the parameters have to be improved with more accurate or precise initial estimates and a tighter or smaller range. The question is which parameter or parameters need to be change?

From the initial variation tests it is observed that VAF and LAMBDA are the two parameters that effect the gradient of the active region which should be low. It is also observed that the level of the collector current can be increased by increasing KP. These three parameters are again varied to get a better initial estimate and optimisation range. In these variation tests all the other parameters are set to the values obtained from the initial optimisation result, except the parameters to be observed namely, LAMBDA, VAF and KP. The range of variation is predicted through trial and error but within the range of the previous discussion.

These three parameters lower the curves in the active region with LAMBDA giving more variation at a lower gate voltage. LAMBDA is varied from 0.001 to 0.1 and the collector current become almost constant in the active region with LAMBDA smaller than 0.001. The decrement of the collector current with the increase in VAF is not so prominent as the case with LAMBDA, even though VAF is varied from 10 to 500. Term KP increased the collector current level to the desired value when it increased to 0.1 and 10.

Following the results above, another optimisation is carried out with LAMBDA fixed at 0.001 and the range for VAF constrained between 50 and 150. Since the collector current is to be increased, the range for KP is increased between 0.1 and 10.0. To simplify the optimisation process further,

the resistance parameters for both the BJT and MOSFET models are left as default values. This is because from the variation test it is observed that these parameters do not show significant effect on the conduction characteristics.

The result of the optimisation is given in Figure 7, and shows the optimised conduction characteristics to be very close to the manufacturer's data. Table 5 lists the value of the static model parameters used for this second optimisation process and the optimised values.

DYNAMIC PARAMETERS

All the dynamic parameters of the BJT and MOSFET model discussed in section III were varied and their effects on the transient characteristics observed. The default values and the variation values for the parameters which affect the transient or switching characteristics are tabulated in Table 6. Each of the dynamic parameters is varied accordingly with the optimised static parameters specified.

From the results obtained, the parameters that determined the switching characteristics are those that specify the junction capacitance of the BJT, and the overlap capacitance and depletion layer capacitance of the MOSFET.

The parameters that specify the junction capacitance of the BJT, being CJC, CJE and CJS very much affect the fall time and the rise time, especially the CJE and CJS. The turn-off delay time increased when the value of CJS is increased. The collector-emitter voltage overshoot is decreased significantly when the parameters CJE and CJS are included in the model. This is due to the longer fall time and hence decrease of the dv/dt rate of the collector-emitter voltage of the BJT model.

TABLE 5. Selected static parameters optimisation with improved estimate

Parameter	Initial estimate, lower limit, upper	Optimised value
IS	659.0406f, le-25, le-12	1.395e-18
BF	500, 10, 1000	10.0000
NF	938.7808m, 0.8, 1.0	1.0000
ISE	1.0693e-22, le-15	1.000e-25
NE	1.2616, 1, 4	4.0000
IKF	99.9967, 1, 200	148.3400
VAF	126.5610, 50, 150	69.9821
RB	default	default
RE	default	default
RC	default	default
VTO	2.6654, 1, 5	4.4548
KP	1.0, 0.1, 10	100.2627m
LAMBDA	fixed at 0.001	0.001
PHI	607.0191m, 0.1, 0.9	900.0000m
GAMMA		986.1898m,
0.1, 1.0	100.0000m	
RS	default	default
RD	default	default

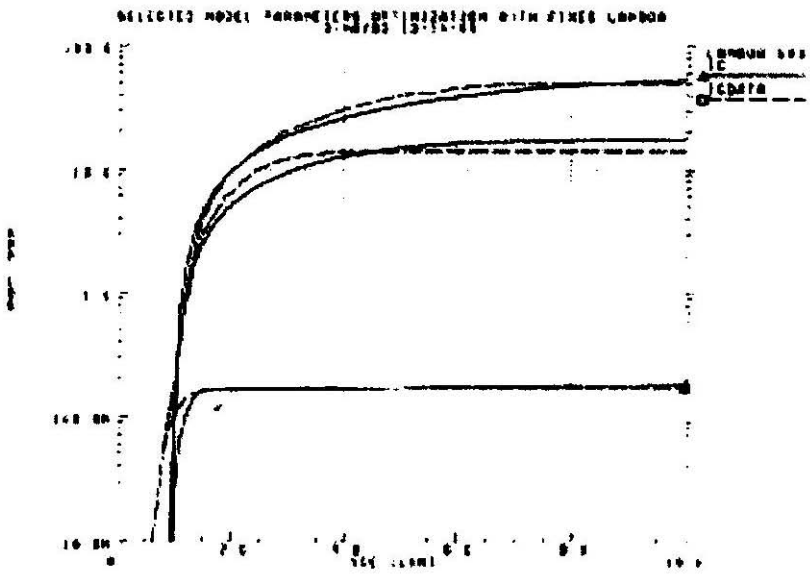

FIGURE 7. Conduction characteristics with static parameter optimised

The overlap capacitance parameters CGBO, CGDO and CGSO have very significant influence on the switching characteristics, especially the fall time. In general, the rate of fall increases with higher values of these parameters, which affect the gate-emitter voltage of the IGBT model and hence the dv/dt rate of the collector-emitter voltage at turn-off. For the depletion layer capacitance only the parameter CBD shows influence on the switching characteristics. The turn-off delay time increased with higher values of CBD.

A clamped resistive-load test, as in Figure 5, was carried out in the laboratory to obtain the switching characteristic of the device. Figure 8 shows some results of the test illustrating the collector-emitter voltage V_{ce} and the gate-emitter voltage V_{ge}, with three different values of gate-emitter resistance R_{ge}. The values used are 270 ohm, 1 Kohm and 2 Kohm. It is observed that with higher values of R_{ge} the delay time is increased and the V_{ce} overshoot is also decreased.

Optimisation of the switching characteristic is based on the data file extracted from the above test with R_{ge} equal to 1 Kohm. Figure 9 shows an

TABLE 6. Default values and values used in variation tests

Parameter	Default value	Variation values
CJC	0	le-12, le-11, le-10
CJS	0	le-9, le-8, le-7
CJE	0	le-8, le-7, le-6
CBD	0	1n, 50n, 100n
CGBO	2e-18	10u, 50u, 100u
CGDO	4e-11	1u, 50u, 100u
CGSO	4e-11	10u, 50u, 100u

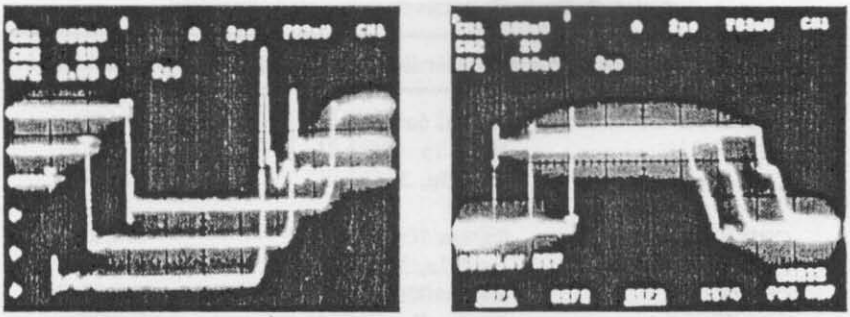

FIGURE 8. Switching circuit test results showing (a) V_{ce} and (b) V_{ge} for R_{ge} of 270 ohm, 1 Kohm and 2 Kohm.

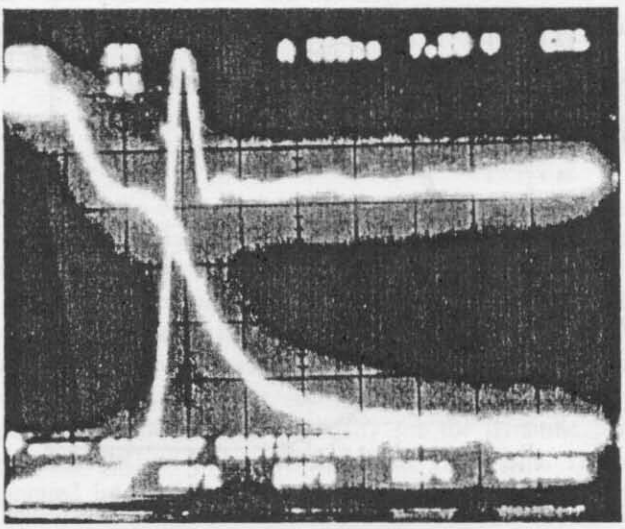

FIGURE 9. Switching circuit test result showing Vce and Vge with Rge of, 1 Kohm

oscillogram of the V_{ce} and the V_{ge}. Based on this experimental result and the variation test results, initial optimisation for the dynamic parameters of the IGBT model was carried out. The initial estimate, the lower limit and the upper limit of each parameter is selected from the variation test. Table 7 lists the values of the dynamic model parameters used for the initial optimisation and the optimised values.

Figure 10 presents the switching characteristics with the initially optimised model parameters. The results show that the collector-emitter voltage dv/dt is lower than the data obtained from the experiment but the fall time of the gate-collector voltage is almost the same as the experimental data. To obtain a better result the optimisation algorithm is run a number of times, using the estimated parameters of the previous run as the initial setting of the next run. This inevitably increases the simulation time.

Figure 11 presents switching characteristics of the device with the selected dynamic parameters optimised after the optimisation algorithm is

TABLE 7. Dynamic parameters initial optimisation

Parameter	Initial estimate, lower limit, upper limit	Optimised value
CJC	4n, 2n, 6n	6n
CJS	100p, 1p, 10n	10n
CJE	1u, 0.5u, 3u	1.3259u
CBD	5n, 1n, 10n	10n
CGBO	1u, 0.7u, 3u	1.9004u
CGDO	300u, 100n, 500n	348.2887n
CGSO	3u, 1u, 5u	3.8989u

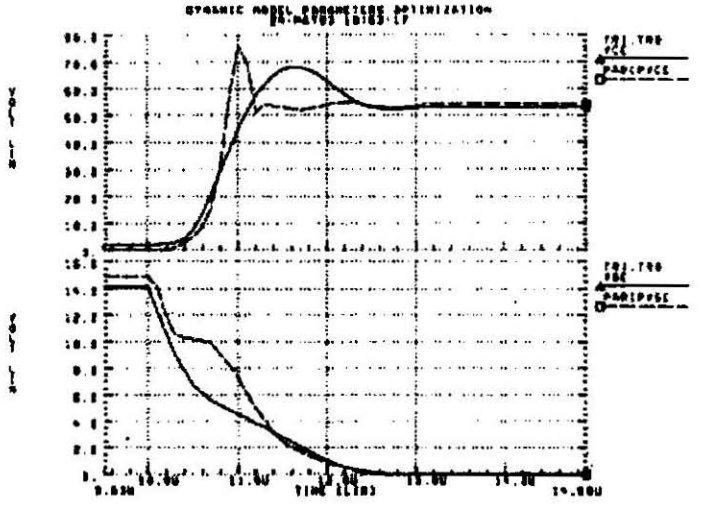

FIGURE 10. Switching characteristics with initially optimised dynamic parameters

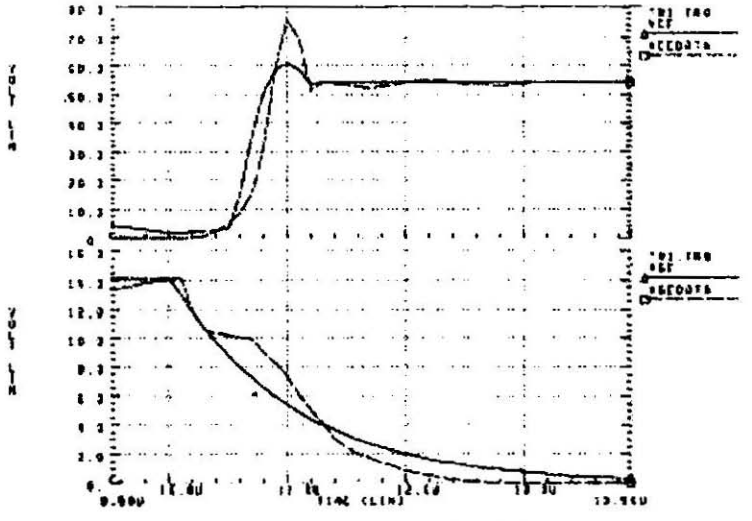

FIGURE 11. Switching characteristics with final optimised dynamic parameters

TABLE 8. Dynamic parameters final optimisation

Parameter	Initial estimate, lower limit, upper limit	Optimised value
CJC	154.4513p, 1p, 100n	42.0069p
CJS	15.4424n, 1p, 100n	115.0816p
CJE	20.7932n, 1p, 100n	81.1413
CBD	26.6324n, 1p, 100n	112.8944p
CGBO	3.5306u, 1p, 10u	4.9972u
CGDO	141.7324n, 1p, 10u	9.6037n
CGSO	1.5349u, 1p, 10u	4.9972u

run a few times. It is observed that a good agreement is then obtained between the experimental output and the simulation data. Table 8 lists the values of the dynamic model parameters used for this final optimisation process and the optimised values.

CONCLUSION

The development of the IGBT model using the HSPICE package is presented. The IGBT model proposed is discussed to give background before a detailed development of the model is presented. The steps in modelling the IGBT using the curve-fitting optimisation method available within HSPICE are explained. Selected device parameters are used in the optimisation algorithm. This generates a set of device parameters based on conduction characteristics data from the manufacturer for the static parameters and switching characteristics data obtained experimentally for the dynamic parameters. The simulation results are comparable with the given data. This model is then incorporated into PECT which is added to the semiconductor device database.

Appendix 1 - BJT Model Parameters

Name	Description	Unit	Default
BF	Ideal maximum forward beta		100.0
BR	Ideal maximum reverse beta		1.0
IBC	Reverse saturation current between base and collector	amp	0
IBE	Reverse saturation current between base and emitter	amp	0
IS	Transport saturation current	amp	1.0e-16
ISS	Reverse saturation current	amp	0
NF	Forward current emission coefficient		1.0
NR	Reverse current emission coefficient		1.0
NS	Substrate current emission coefficient		1.0
SUBS	Substrate connection selector		1.0
BULK	Sets the bulk node to a global node name		0
ISC	Base-collector leakage saturation current	amp	0
ISE	Base-emitter leakage saturation current	amp	0
NC	Base-collector leakage emission current		2.0
NE	Base-emitter leakage emission current		1.5
IKF	Corner for forward beta high current roll-off	amp	0
IKR	Corner for reverse beta high current roll-off	amp	0
VAF	Forward early voltage	volt	0
VAR	Reverse early voltage	volt	0
IRB	Base current where base resistance falls half-way to RBM	amp	0
RB	Base resistance	ohm	0
RBM	Minimum high current base resistance	ohm	RB
RE	Emitter resistance	ohm	0
RC	Collector resistance	ohm	0
CJC	Base collector zero bias depletion capacitance	farad	0
CJE	Base emitter zero bias depletion capacitance	farad	0
CJS	Zero bias collector substrate capacitance	farad	0
FC	Coefficient for forward bias depletion capacitance formula		0.5
MJC	Base-collector junction exponent		0.33
MJE	Base-emitter junction exponent		0.33
MJS	Substrate junction exponent		0.5
VJC	Base collector built in potential	volt	0.75
VJE	Base-emitter built in potential	volt	0.75
VJS	Substrate junction built in potential	volt	0.75
XCJC	Internal base fraction of base-collector depletion capacitance		1.0
CBCP	External base-collector constant capacitance	farad	0
CBEP	External base-emitter constant capacitance	farad	0
CCSP	External collector substrate constant capacitance	farad	0
ITF	TF high current parameter	amp	0
PTF	Frequency multiplier to determine excess phase	degree	0
TF	Base forward transit time	sec	0
TR	Base reverse transit time		
TF	base collector voltage dependence coefficient	sec	0
VTF	TF base-collector voltage dependence coefficient		0
XTF	TF bias dependence coefficient		0
AF	Flicker noise exponent		1.0
KF	Flicker noise coefficient		0

Appendix 2 - MOSFET LEVEL=1 Model parameter

Name	Description	Unit	Default
ACM	Area calculation method		2
JSW	Side wall bulk junction saturation current	amp/m	0
IS	Bulk junction saturation current	amp	1e-14
N	Emission coefficient		1
NDS	Reverse bias slope coefficient		1
CBD	Zero-bias bulk drain junction capacitance	farad	0
CBS	Zero-bias bulk source junction capacitance	farad	0
CJ	Zero-bias bulk junction capacitance	F/m^2	0
CJSW	Zero-bias side wall junction capacitance	F/m	0
FC	Forward bias depletion capacitance coefficient		0.5
MJ	Bulk junction grading coefficient		0.5
MJSW	Bulk side wall junction grading coefficient		0.33
NSUB	Substrate doping	$1/cm^3$	1e15
PB	Bulk junction contact potential	volt	0.8
PHP	Bulk side wall junction contact potential	volt	PB
TT	Transit time	second	0
RD	Drain ohmic resistance	ohm	0
RDC	Additional drain resistance due to contact	ohm	0
RS	Source ohmic resistance	ohm	0
RSC	Additional source resistance due to contact	ohm	0
RSH	Drain and source diffusion sheet resistance	ohm/sq.	0
LD	Lateral diffusion into channel	m	0
LMLT	Length shrink factor		1
WD	Lateral diffusion into channel from bulk	m	0
WMLT	Diffusion layer and width shrink factor		1
XJ	Metallurgical junction depth	m	0
XL	Length masking and etching effects	m	0
XW	Width masking and etching effects	m	0
GAMMA	Body effect factor	$V^{1/2}$	0.5276
NFS	Fast surface state density	cm^{-2}	0
NSUB	Bulk surface doping	cm^{-3}	1e15
PHI	Surface inversion potential	V	0.576
VTO	Zero bias threshold voltage	V	0
ALPHA	Impact ionisation current coefficient	1/V	0
VCR	Critical voltage	V	0
COX	The oxide capacitance per unit gate area	F/m^2	3.453e-4
LEVEL	DC model selector		1
KP	Intrinsic conductance parameter	amp/V^2	
LAMBDA	Channel length modulation	1/V	0
TOX	The oxide thickness	m	1e-7
UO	Carrier mobility	$cm^2/V.s$	
CGBO	Gate-bulk overlap capacitance/meter length	F/m	0
CGDO	Gate-drain overlap capacitance/meter length	F/m	0
CGSO	Gate-source overlap capacitance/meter length	F/m	0
METO	Fringing field factor	m	0
AF	Flicker noise exponent		1
KF	Flicker noise coefficiet		0
NLEV	Noise equation selector		2

REFERENCES

Antognetti, P. 1988. *Semiconductor Device Modelling with SPICE.* New York: McGraw Hill.

Baliga, B. J., Adler, M. S., Love, R. P., Gray, P. V., and Zommer N. D. 1984. The insulated gate transistor: A new three-terminal MOS-controlled bipolar power device. *IEEE Trans. on Electron Device,* ED-31(6).

Banzhaf, W. 1989. *Computer-Aided Circuit Analysis Using SPICE.* Engelwood Cliff: Prentice Hall.

Clemente, S., Dubhashi, A. & Pelly, B. 1991. IGBT characteristics and applications, *IGBT Designer's Manual,* 2nd Edition. International Rectifiers.

Cumbi, M. J. N., Shepherd, D. W. & Hulley, L. N., 1996. Develpment of an object-oriented knowledge-based system for power electronic circuit design, *IEEE Trans Power Electronics* 11(3): 393-404.

Hefner, A. R. 1990. Analytical modelling of device - circuit interaction of for the Power Insulated Gate Bipolar Transistor (IGBT). *IEEE Trans. on Industry Applications* 26(6).

Hefner, A. R. 1991. An investigation of the drive circuit requirements for the power Insulated Gate Bipolar Transistor (IGBT). *IEEE Trans. on Power Electronics* 6(2).

Hefner, A. R. & Diebolt, D. M. 1994. An experimentally verified IGBT model implemented in the Saber Circuit Simulator. *IEEE Trans. on Power Electronics* 9:532.

Kaplan, G. 1998. Industrrial electronics technology 1998. Analysis and forecast. *IEEE Spectrum* 35(1): 73-78.

Lauritzen, P. O. 1988. Simulation and modelling for power electronics, *Proc. Of IEEE Workshop on Computers in Power Electronics:* Cambridge MA, USA.

Mariun, N. B. 1997. Knowledge Based Expert System for power electronics design. PhD Thesis, Dept. of Electronic and Electrical Engineering, Uni. of Bradford, UK.

Malik, N. R. 1990. Determining SPICE Parameters Values for BJTs. *IEEE Trans. on Education* 33(4).

Meta-Software Inc. 1990. *HSPICE User's Manual H9001.*

Rashid, M. H. 1990. *SPICE for Circuits and Electronics Using SPICE.* Englewood Cliff: Prentice Hall.

Tuinenga, P. W. 1988. *A Guide to Circuit Simulation and Analysis Using SPICE.* Englewood Cliff : Prentice Hall.

Yilmaz, H., Van Dell, W. R., Owyang, K., and Chang, M. F. 1985. Insulated Gate Transistor Physics: Modelling and optimization of the on-state characteristics. *IEEE Trans. on Electron Device,* ED-32(1).

Norman bin Mariun and Ishak bin Aris
Dept. of Electrical and Electronic Engineering
Universiti Putra Malaysia
43400 UPM Serdang, Selangor D.E. Malaysia

D. Liang and W. Shepherd
Dept. of Electronic and Electrical Eng.
University of Bradford
BD7 1DP, United Kingdom